Brewster's Scattering Angle in Scattered Waves from Slightly Rough Metal Surfaces

Tetsuya Kawanishi
Communications Research Laboratory, Ministry of Posts and Telecommunications, 4-2-1 Nukui-Kitamachi, Koganei, Tokyo 184-8795, Japan
(Received 24 August 1999)

Brewster's scattering angle in electromagnetic wave scattering from slightly random metal surfaces is investigated by means of the stochastic functional approach. While there are dips due to Brewster's scattering angle in scattering profiles from dielectric surfaces, Brewster's scattering angle does not exist in scattering from metal surfaces. However, the dips can exist in scattering from rough metal surfaces with the optically denser medium to convert evanescent wave into radiative wave.

PACS numbers: 42.25.–p, 46.65.+g

In random scattering from rough surfaces, several interesting features have been clarified such as anomalous scattering, backscattering enhancement, and memory effect [1–7]. Recently, the present author has successfully formulated electromagnetic wave scattering from a random dielectric surface, and has described several specific phenomena, such as quasianomalous scattering and Brewster's scattering angle [8,9]. In this Letter, Brewster's scattering angle in scattered waves from metal surfaces is investigated. In the case of random scattering from a dielectric surface, Brewster's scattering angles where scattering profiles have a dip exist in p-polarized scattering, and depend on the refractive index of the dielectric and on the incident angle. The first order scattering intensity at the dip is equal to zero, if the dielectric is lossless. On the other hand, when the scatterer is a metal surface, there is no real solution to the equation which gives Brewster's scattering angle. We show that there are zeros in the first order scattering, when a part or all of the scattering process is evanescent. Therefore, by introducing an optically denser medium, which can convert an evanescent wave at the random surface into a radiative wave, the dip due to Brewster's scattering angle can be seen in the scattering profiles in the optically denser medium.

Consider the scattering structure as shown in Fig. 1. The incident wave from the side labeled Med. 1 illuminates a random interface between Med. 1 and Med. 2, which denote the upper and lower media with respect to the random surface. The incident plane wave comes from the direction (θ_0, ϕ_0), where θ_0 and ϕ_0 denote, respectively, the zenith and the azimuth angles. Similarly, (θ_s, ϕ_s) denotes the scattering direction. In this Letter, we use the coordinate in which the incident plane corresponds to the xz plane, i.e., $\phi_0 = 0°$. In the p-polarized scattered wave intensity distributions on the incident plane produced by the p-polarized incidence, there are zeros in the incident plane. In Med. 1, the zero exists at

$$\theta_s = \Theta_{B1} \equiv \sin^{-1}\left[n \sin\left\{ \tan^{-1}\left(\frac{1}{n^2 \tan[\sin^{-1}(n^{-1}\sin\theta_0)]} \right) \right\} \right], \qquad \phi_s = 0°, \tag{1}$$

which corresponds to Brewster's scattering angle, where n denotes the refractive index of Med. 2 with respect to Med. 1 [8].

Consider the case of scattering from a metal surface. For simplicity, the refractive index of Med. 2 is assumed to be a pure imaginary number, $n = i\alpha$, in the visible ray region. The refractive index of low-loss metal can be approximately expressed by a pure imaginary number. When n is a pure imaginary number, Brewster's scattering angle Θ_{B1} is a complex number, corresponding to an evanescent wave. On the other hand, when the incident wave is evanescent, Θ_{B1} may be a real number. Therefore, the incident wave or the scattered wave should be evanescent to observe Brewster's scattering angle, and it is impossible to see the dip of Brewster's scattering angle from far field in the scattering distribution produced by incidence from far field. The third medium (Med. 3) is introduced to convert the evanescent wave into a radiative wave which can propagate to far field (see Fig. 2). The refractive index of Med. 3 with respect to Med. 1 is denoted by n_g and is larger than unity. By using Eq. (124) in Ref. [8] and Snell's law

$$n_g \sin\theta_{0m} = \sin\theta_0, \qquad n_g \sin\Theta_{Bm} = \sin\Theta_{B1}, \tag{2}$$

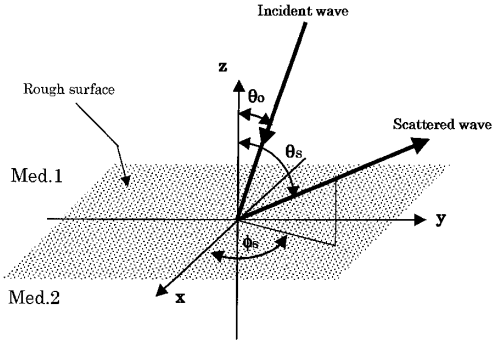

FIG. 1. Coordinate system for random scattering from rough surface.

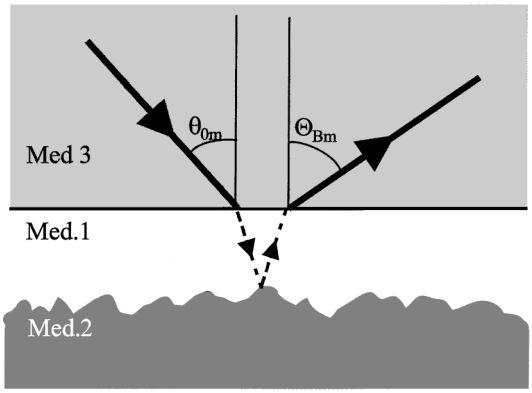

FIG. 2. Scattering structure of rough metal surface with optically denser medium.

where θ_{0m} denotes the incident angle in Med. 3, we get the expression for Brewster's scattering angle in Med. 3 as follows:

$$\Theta_{Bm} = \sin^{-1}\left[\frac{\alpha}{n_g}\sqrt{\frac{n_g^2\sin^2\theta_{0m} + \alpha^2}{n_g^2\sin^2\theta_{0m}(\alpha^4 - 1) - \alpha^2}}\right]. \quad (3)$$

In Fig. 3, Brewster's scattering angles Θ_{Bm} are shown as functions of the incident angle θ_{0m}. When the incident angle θ_{0m} is smaller than the critical angle $\theta_c = \sin^{-1}(1/n_g)$, the rough surface is illuminated by a radiative wave in Med. 1 and Brewster's scattering angle in Med. 1, Θ_{B1}, always corresponds to an evanescent wave; that is, Brewster's scattering angle in Med. 3, Θ_{Bm}, is larger than θ_c. On the other hand, when θ_{0m} is larger than θ_c, the rough surface is illuminated by an evanescent wave in Med. 1 and Θ_{B1} may correspond to a radiative wave in Med. 1; that is, Θ_{Bm} may be smaller than θ_c. Thus, Eq. (3) means that Brewster's scattering angle can exist only in the following three cases: (1) incident wave is radiative, but scattered wave is evanescent, (2) incident wave is evanescent, but scattered wave is radiative, (3) both incident and scattered waves are evanescent. In other words, a part or all of the scattering process which shows Brewster's scattering angle is always evanescent.

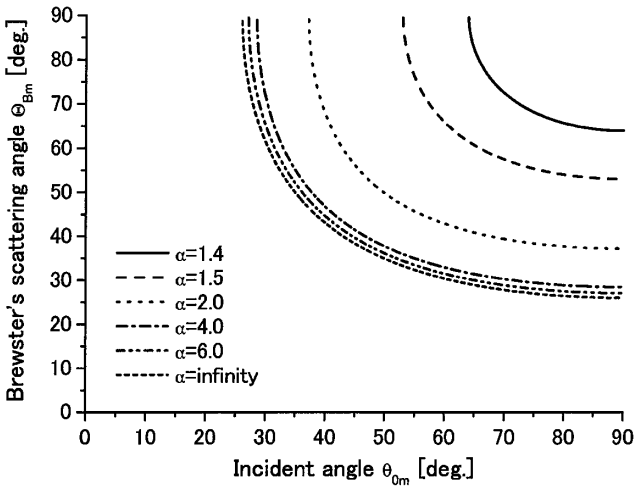

FIG. 3. Brewster's scattering angles in scattering from metal surfaces, where $n_g = 1.51$ and $\theta_c = 41.47°$.

In addition, at the limit of $\alpha \to \infty$, Θ_{Bm} is always smaller than θ_c on the condition of $\theta_{0m} > \theta_c$. When α is small, Θ_{Bm} does not exist in radiative wave in Med. 3. When α is large, the curves for various α do not depend on α very much, and at the limit of $\alpha \to \infty$, Θ_{Bm} is equal to $\sin^{-1}[1/n_g^2\sin\theta_{0m}]$.

If the multiple scattering effects are ignored, the p-polarized scattered wave of the scattering structure in Fig. 2 can be expressed by the first order Wiener kernels A_1^H and A_1^V [see Eqs. (106)–(114) in Ref. [8]] as follows:

$$T_1^H E_1 A_1^H E_2 T_2^H, \quad \text{for } s\text{-polarized scattering}, \quad (4)$$

$$T_1^V E_1 A_1^V E_2 T_2^V, \quad \text{for } p\text{-polarized scattering}, \quad (5)$$

where

$$T_1^H \equiv \frac{2n_g\cos\theta_{0m}}{n_g\cos\theta_{0m} + \sqrt{1 - n_g^2\sin^2\theta_{0m}}},$$

$$T_2^H \equiv \frac{2\sqrt{1 - n_g^2\sin^2\theta_{sm}}}{n_g\cos\theta_{sm} + \sqrt{1 - n_g^2\sin^2\theta_{sm}}}, \quad (6)$$

$$T_1^V \equiv \frac{2n_g\cos\theta_{0m}}{\cos\theta_{0m} + n_g\sqrt{1 - n_g^2\sin^2\theta_{0m}}},$$

$$T_2^V \equiv \frac{2\sqrt{1 - n_g^2\sin^2\theta_{sm}}}{\cos\theta_{sm} + n_g\sqrt{1 - n_g^2\sin^2\theta_{sm}}}, \quad (7)$$

$$E_1 \equiv \exp[ikd\sqrt{1 - n_g^2\sin\theta_{0m}}],$$

$$E_2 \equiv \exp[ikd\sqrt{1 - n_g^2\sin\theta_{sm}}]. \quad (8)$$

T_1^H, T_1^V and T_2^H, T_2^V denote the Fresnel's transmission coefficients on the Med. 1 and Med. 3 interface of the incident wave and the scattered wave, respectively. E_1 and E_2 are the attenuation coefficients due to the decay of the evanescent wave in Med. 1. θ_{0m} and θ_{sm} denote the incident and the scattering angle in Med. 3. k and d mean, respectively, the wave number in Med. 1 and the thickness of Med. 1. The rough surface is assumed to be a homogeneous Gaussian random field, as shown in Ref. [8]. When the thickness d is larger than the incident wavelength, the intensity of the scattered wave around Brewster's scattering angle is very small due to the decay of evanescent wave, so that it is difficult to detect the dip of Brewster's scattering angle. In addition, when the thickness d is not larger than the roughness of the interface between Med. 1 and Med. 2, Med. 2 may intersect Med. 3, and the model of the three-layered scattering structure shown in Fig. 2 is no longer valid. Thus, we should choose the thickness d to be larger than the roughness and smaller than the wavelength. For numerical calculation, the following assumptions are made: $n = 0.97 + 6.00i$ (Al at 633 nm), $n_g = 1.51$ (crown glass), $k\sigma = 0.03$, $kl = 1.0$, and $kd = 1.0$, where σ and l denote roughness and

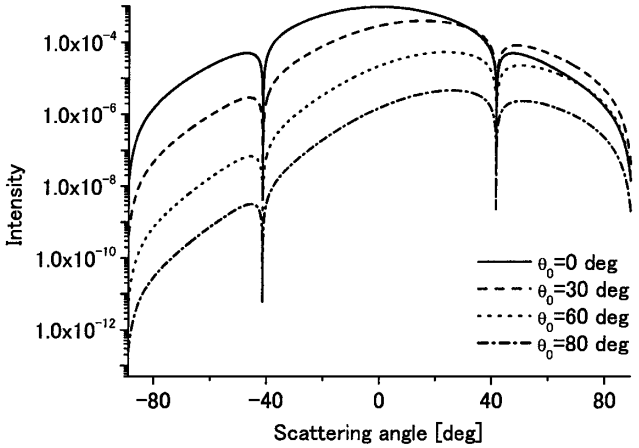

FIG. 4. Scattering profile for s-polarized incident.

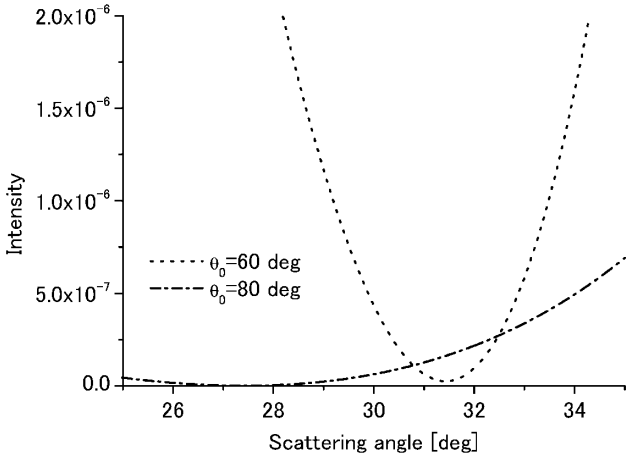

FIG. 6. Blowup of Fig. 5 at 30°.

correlation length of the interface between Med. 1 and Med. 2. Figure 4 shows the scattering profiles of s-polarized scattering induced by s-polarized incidence. Figure 5 shows the scattering profiles of p-polarized scattering induced by p-polarized incidence. In both the s- and p-polarized scattering profiles, there are dips at the critical angle of total reflection for Med. 1 and Med. 3 interface. This is because the transmittance T_2 equals zero at this angle. Peaks in p-polarized scattering are due to the surface plasmon mode on the Med. 1 and Med. 2 interface. When $\alpha = 6.0$ is substituted in Eq. (3), Brewster's scattering angles of the structure as shown in Fig. 2 are obtained. Θ_{Bm} for $\theta_{0m} = 30°$, $\theta_{0m} = 60°$, and $\theta_{0m} = 80°$ equal, respectively, 65.07°, 31.52°, and 27.51°. As shown in Fig. 5, there are dips due to Brewster's scattering angle in the p-polarized scattering angle, but no dips in the s-polarized scattering profile in Fig. 4. The directions of the dips for $\theta_{0m} = 30°$, $\theta_{0m} = 60°$, and $\theta_{0m} = 80°$ are 64.86°, 31.43°, and 27.43° (see Figs. 6 and 7). Brewster's scattering angle for a metal surface with loss is smaller than that for lossless metal. The shift of Brewster's scattering angle due to the loss is investigated by calculating p-polarized scattering profiles and varying the loss of the metal. In Fig. 8, Brewster's scattering angle, which is the direction of the dip in the scattering profile, and the scattering intensity at Brewster's scattering angle are shown as a function of β defined by $n = 0.97\beta + 6.0i$. When the loss of the metal is increased, Brewster's scattering gets smaller and the scattering intensity at the bottom of the dip becomes larger. However, the shift of Brewster's angle is not very large, so that the expression of Eq. (3) can be used in approximate estimations for actual metal surfaces. If we detect a shift of Brewster's scattering angle or the scattering intensity at the dip, the loss of the metal surface can be estimated by comparing the shift with the simulated data as shown in Fig. 8. In addition, Fig. 9 shows Brewster's scattering angle and the scattering intensity at Brewster's scattering angle as a function of the argument of the refractive index. The modulus of the refractive index is assumed to be 6.0. The cases of the argument $\theta = 0°$, 45°, and 90° correspond, respectively, to lossless dielectric, conductor,

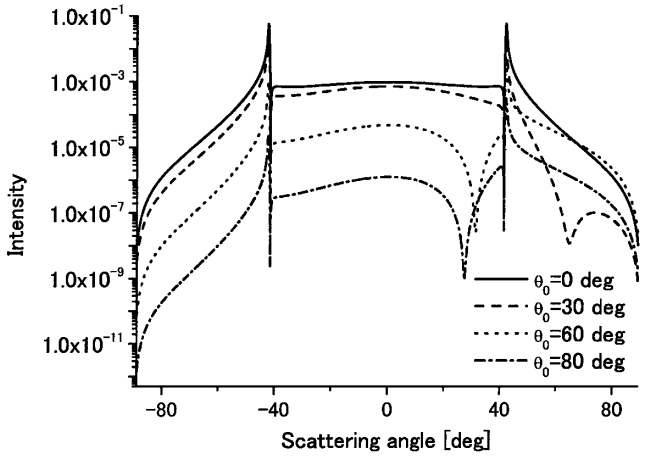

FIG. 5. Scattering profile for p-polarized incident.

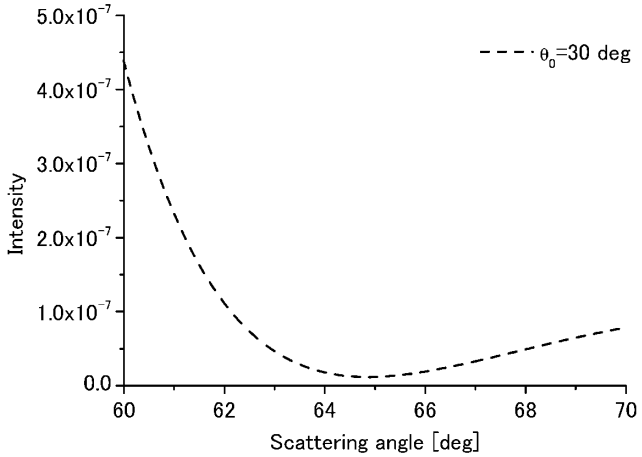

FIG. 7. Blowup of Fig. 5 at 65°.

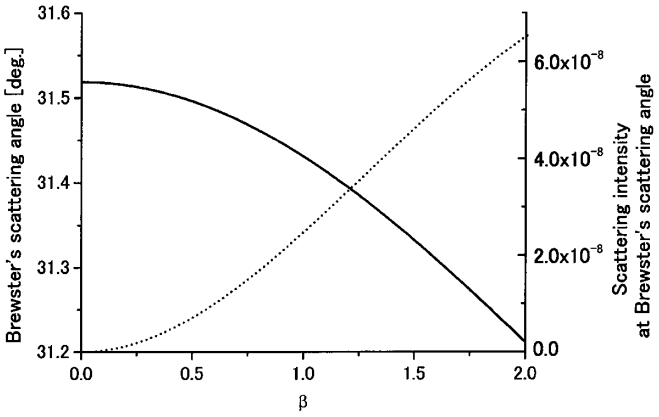

FIG. 8. Shift of Brewster's scattering angle for $\theta_{0m} = 60°$. Solid line and dashed line denote Brewster's scattering angle and the scattering intensity at Brewster's scattering angle, respectively.

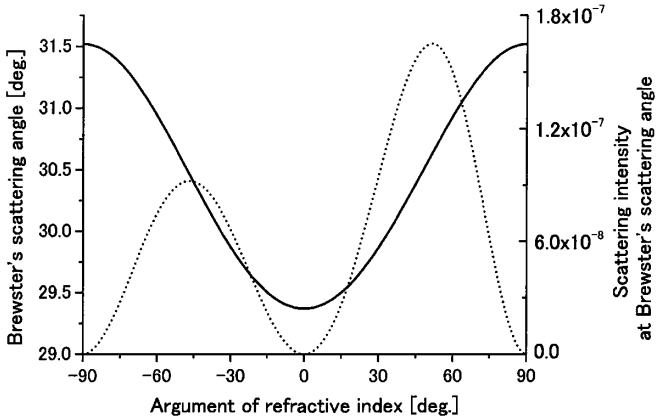

FIG. 9. Shift of Brewster's scattering angle for $\theta_0 = 60°$ as a function of argument of n. Solid line and dashed line denote Brewster's scattering angle and the scattering intensity at Brewster's scattering angle, respectively.

and lossless metal. $\theta < 0$ means Med. 2 has gain. Brewster's scattering angle has the minimum at $\theta = 0°$ and the maximum at $\theta = \pm 90°$, so that the shift Brewster's scattering angle of dielectric surfaces due to the loss of the medium is positive, while that of metallic surfaces is negative. The curve for Brewster's scattering angle is symmetric with respect to $\theta = 0°$, but the scattering intensity in $\theta < 0°$ is smaller than in $\theta > 0°$. The scattering intensity goes to zero at $\theta = 0°$ and 90° which correspond to lossless media, and has the maximum near $\theta = 45°$ which corresponds to a conductor. The zeros at Brewster's scattering angle can exist in the first order scattering not only from lossless dielectric but also from lossless metal.

In conclusion, the light scattering from metal surfaces is studied by means of the stochastic functional approach. This Letter has shown that a part or all of the scattering process which shows Brewster's scattering angle is always evanescent, and that the dip corresponding to Brewster's scattering angle can be observed by introducing an optically denser medium to convert evanescent wave into radiative wave. Brewster's scattering angle shift due to loss of the metal surface has been shown to be always negative.

This author expresses appreciation to Professor H. Ogura and Dr. M. Izutsu for their encouragement.

[1] Y. Q. Jin and M. Lax, Phys. Rev. B **42**, 9819–9829 (1990).
[2] M. E. Knotts and K. A. O'Donnell, Opt. Commun. **99**, 1–6 (1993).
[3] A. Ishimaru, J. S. Chen, P. Phu, and K. Yoshitomi, Waves Random Media **1**, 91–107 (1991).
[4] A. R. McGurn and A. A. Maradudin, J. Opt. Soc. Am. B **4**, 910–926 (1985).
[5] V. Celli, A. A. Maradudin, A. M. Marvin, and A. R. McGrun, J. Opt. Soc. Am. A **2**, 2225–2238 (1985).
[6] H. Ogura and Z. L. Wang, Phys. Rev. B **53**, 10 358–10 371 (1996).
[7] T. Kawanishi, Zhi Liang Wang, and Masayuki Izutsu, J. Opt. Soc. Am. A **16**, 1342–1349 (1999).
[8] T. Kawanishi, H. Ogura, and Z. L. Wang, Waves Random Media **7**, 351–384 (1997).
[9] T. Kawanishi, I. Iwata, M. Kitano, H. Ogura, Z. L. Wang, and M. Izutsu, J. Opt. Soc. Am. A **16**, 339–342 (1999).